J Porous Mater
DOI 10.1007/s10934-012-9633-7

Two modes in macroporous Cu_2O growth through template-assisted electrodeposition method

Yanbo Ding · Lili Yang · Yao Li · Xiaohong Wu · Yueye Lu · Jiupeng Zhao

Abstract Macroporous materials with three dimensional pores and channels are anticipated to exhibit improved performance in numerous applications such as photonic band gap crystals, battery electrodes and gas sensors due to their special structure. In this work, macroporous Cu_2O thin films were prepared by template-assisted electrodeposition method. The mechanism of electrodeposition infiltrating procedures indicated that the target architectures can basically maintain its original shape, and the fabrication of spherical-porous shaped Cu_2O controlled by crystalline structures is firstly studied systematically. The morphology of macroporous material along the (1 1 1) direction demonstrated that the target architecture can copy both the crystalline structures and the colloidal crystal template. Moreover, models are set up to discuss the evolution of the morphology (the shapes of the pore mouths and pore walls), which indicated that the pore mouths and pore walls were deeply influenced by the deposition depth.

Y. Ding · J. Zhao (✉)
School of Chemical Engineering and Technology,
Harbin Institute of Technology, Harbin 150001, China
e-mail: jiupengzhao@126.com

Y. Ding · X. Wu
School of Science, Harbin Institute of Technology,
Harbin 150001, China

L. Yang
School of Transportation Science and Engineering,
Harbin Institute of Technology, Harbin 150090, China

Y. Li · Y. Lu
Center for Composite Materials and Structures, Harbin Institute
of Technology, Harbin 150080, China

Published online: 26 September 2012

Keywords Cu_2O thin films · Electrodeposition · Ordered macroporous · Template assistant

1 Introduction

Much attention has been attracted to three-dimensionally ordered macroporous (3DOM) materials with uniform pore size and well-defined periodic structure due to their potential applications, such as catalyst supports, adsorption, separation, catalysts, sensors, photonic crystals, lithium batteries [1–7]. Thanks to the efforts from a large number of research groups, a myriad of inverse opal structure materials such as carbon, Au, to transition metal oxides and complex oxides [8–11] which possesses the high surface-to-volume ratio, well-defined pore dimensions and precisely controlled structures have been prepared. Among the various fabrication methods have been reported [12], the method using colloidal crystals as templates is comparably simple and efficient. The morphology and thickness of macroporous film can be easily controlled via simply adjusting the electrochemical parameters such as current, potential, or deposition time. Most important, it is a bottom-up deposition technique and allows a high filling ratio of materials in the interstice of the template because the macroporous film grows upwards from the conductive substrate which fill the template completely. To all of us knows, the quality of the colloidal crystals pay a very important role in determine the target architectures, and the effect of template on the structure of inverse opals have been reported [13, 14]. However, the influence of the crystalline structure in the formation of duplicated architectures hasn't been well considered or studied. Therefore, there is an urgent need to develop the effects of the crystalline structure in the formation of constructing macroporous and 3DOM materials.

Cu_2O is an important transition metal oxide with potential applications across a number of technological fields. Being a p-type oxide semiconductor with a direct band gap of 2.17 eV, Cu_2O has been found in applications of solar energy utilization, chemical and biosensing, photon-activated water splitting, low temperature CO oxidation, photodegradation of organic pollutants, micro- and nanoelectronics, and magnetic storage devices [15–17] etc. Because of its technological importance, morphology controlled synthesis of Cu_2O micro- and nanostructures have received considerable attention in recent years [18, 19]. Herein, we report a facile way for controllable fabrication of shaped macroporous Cu_2O by electrochemical deposition via simply adjusting the electrochemical deposition voltage. The interest here focuses on the disordered crystal configuration during the electrochemical deposition. The experimental results show that there are two types of growth modes in which close-packed macroporous Cu_2O at -0.35 V and spherical-porous Cu_2O clusters are obtained at -0.38 or -0.42 V copying from the colloidal crystals template and distorted crystalline structure. To the very best of our knowledge, this is the first report about the shaped macroporous fabrication controlled by crystalline structures. The detailed discussion focused on the evolution of the morphology of the spherical-shaped macroporous and the relationship between the shape of the pore mouths and the deposition depth.

2 Experiment

2.1 Materials

The starting materials used were styrene (C_8H_8), potassium persulfate ($K_2S_2O_8$), cupric sulfate ($Cu_2SO_45H_2O$), lactic acid ($C_3H_6O_3$), sodium hydroxide (NaOH) and tetrahydrofuran (C_4H_8O). All these chemicals are analytical reagents. Water used in all experiments was purified with a resistivity greater than 18 M Ω/cm. Glass slides coated with ITO (indium tin oxide) (Rs = 30 Ω) were all commercially available products. ITO/glass was washed with acetone, ethanol, and deionized water for 20 min, respectively, under sonication before use. Other materials were used without further purification.

2.2 Fabrication of PS colloidal crystal templates

Monodispersed PS spheres with an average diameter of (570 ± 10 nm) and relative standard deviation smaller than 4 % (on the diameter) were obtained by using an emulsifier-free emulsion polymerization technique [20]. ITO (10 × 30 mm) was used as substrates for PS template growth. PS colloidal crystals were grown by using controlled vertical drying deposition method, which has been previously reported [21]. The substrate was placed in a vial containing 0.2 wt% PS colloidal suspensions with a tilt angle of about 65°. The vial was then heated in an incubator at 60 °C until the solvent was completely evaporated, well ordered templates are robust and adhere well to the substrates and appear distinct colors after the slowly evaporated.

2.3 Fabrication of Cu_2O macroporous materials and their characterization

The Cu_2O 3D ordered macroporous materials were constructed by electrochemical deposition of copper (II) lactate in alkaline solution [22]. The electrolyte solution consisted of 0.4 M $CuSO_4$ and 3 M lactic acid and the pH of the solution was adjusted to 9 by 8 wt% NaOH solution. Cu_2O was grown potentiostatically in a three-electrode system controlled by CHI660C station. ITO substrates covered PS colloidal crystal was used as the working electrode with a Pt counter electrode and a saturated calomel reference electrode (SCE). The electrodeposition was performed for 30 min and the deposition temperature was kept constant at 60 °C. The Cu_2O 3D macroporous materials were obtained after removing PS in THF solution.

The morphologies of the PS colloidal crystals and Cu_2O 3DOM materials were performed using a QUANTA200F SEM (FEI, American) scanning electron microscope operating at an accelerating voltage of 30 kV. The samples were sputter-coated with gold before examination.

3 Result and discussion

3.1 Morphologies of macroporous Cu_2O

Figure 1 shows top-viewed SEM images of flat Cu_2O film, well-ordered colloidal crystal and 3D ordered macroporous Cu_2O structure. The flat Cu_2O film was obtained by electrodeposition at -0.35 V versus SCE as show in Fig. 1a. The pores were well ordered in the fcc close-packed structure after removing the template with the well-ordered colloidal crystals were used as templates, which was consistent with the (111) plane arrangement of fcc structure as shown in Fig. 1c. Cu_2O was grown homogeneously in the template and the top of the 3DOM Cu_2O material shows a smooth and flat plane due to the same diffusion rate of the reactants in each channel of the well-ordered structure. According to theoretical analysis, point windows should be left around the regions where the original spheres were in contact when the deposition (infiltration) is complete. Contemporarily, connections are generated for polymeric sphere during the self-assembly process thus leading to larger pore windows rather than point windows.

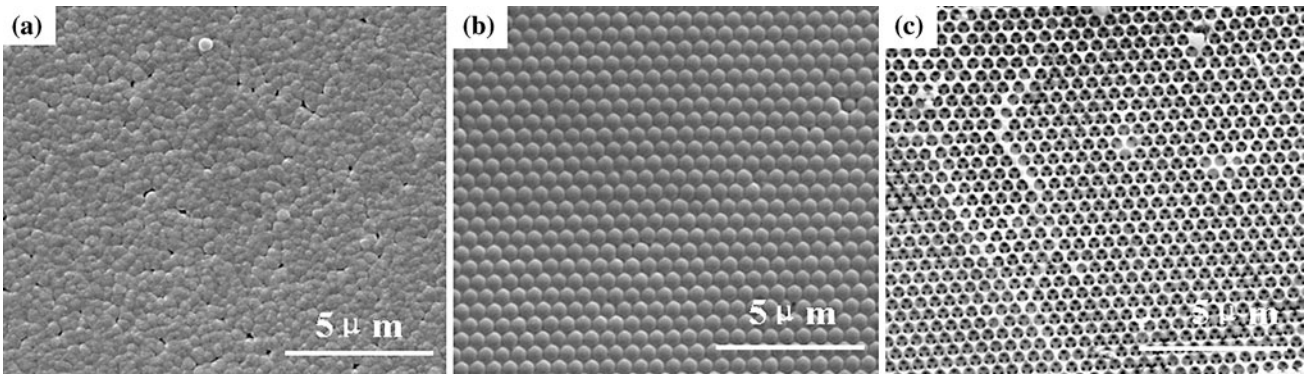

Fig. 1 SEM images of **a** flat Cu_2O film; **b** well-ordered PS colloidal crystal templates; **c** 3D ordered macroporous Cu_2O structure

The synthesis of the structured macroporous films was carried out by the electrodeposition via simply adjusting the voltage within the interstitial spaces of close packed polystyrene latex sphere templates. Pore-free Cu_2O film was obtained on the bare ITO substrate in a controlled experiment when the electrodeposition voltage was adjusted to −0.38 V versus SCE as show in Fig. 2a. It is obviously seen that the Cu_2O film intended to form cluster-shape instead of flat film. Figure 2b presents typical SEM images of the porous Cu_2O crystals obtained by templating of latex particles with followed by THF extraction. There are two typical kinds of pore contours (flat and sphere-like) as show by arrows. The flat areas of Cu_2O crystallite after infiltrating demonstrate evenly porous morphology. However, the cluster part exhibit spherical-pore with a distributed surface pores as show by arrows, which indicated that Cu_2O can basically maintain its original shape when it grows in the interstices among the microspheres of the template, apparently. Those Cu_2O clusters were believed to be grown directly from the space of the colloidal crystals on the ITO substrate, which preferentially nucleated on the latex particles and grew into Cu_2O-coated latex particles.

Figure 3 shows the morphonology of Cu_2O film and their inverse opal prepared by electrodeposition at −0.42 V

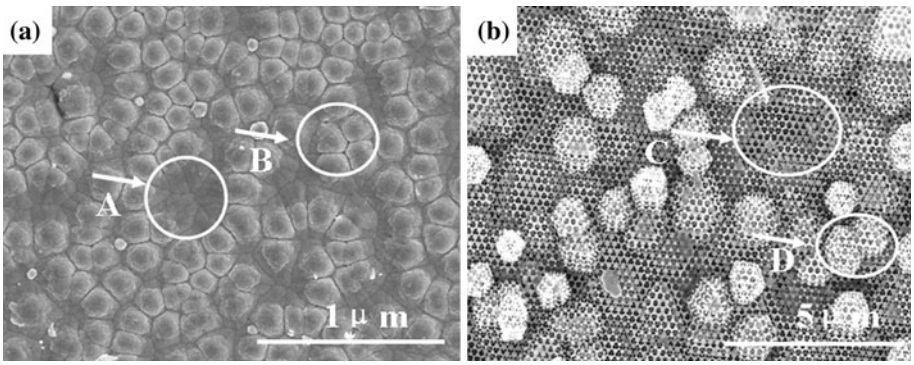

Fig. 2 SEM images of **a** Morphonology of Cu_2O film electrodeposited at −0.38 V versus SCE; **b** Cross-sectional SEM image of macroporous Cu_2O structure

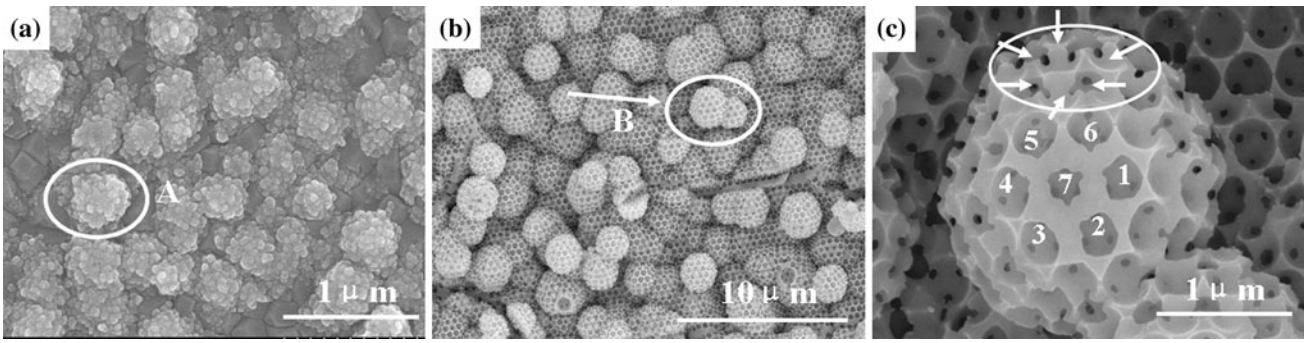

Fig. 3 **a** The morphonology of Cu_2O film electrodeposited at −0.42 V versus SCE; **b** Template-assistant microporous Cu_2O electrodeposited at −0.42 V versus SCE; **c** The magnification images of the spherical pores

versus SCE. It is obviously seen that the Cu_2O film form larger clusters spread all over the ITO. The spherical-porous Cu_2O cluster obtained by templating of latex particles with followed by THF extraction. The image shows that the voids left in the Cu_2O film after removal of the template are arranged in well ordered circular openings shown in Fig. 3c. Interestingly, the circular of pore accompany with bowl-like and distorted pore can be obtained. While the Cu_2O crystal was thoroughly perforated by 3D interconnected ordered macropores. Experimental results indicate that the morphology of shaped Cu_2O macroporous materials is closely related to the infiltration crystalline architecture. The mechanism of the infiltration procedures and the formation of pores mouth will be discussed in the following part.

3.2 Growth modes during the formation of porous Cu_2O

The schematic illustration of infiltrating procedure based on PS colloidal crystal as show in Fig. 4. On the basis of the above observations, a possible formation process of the spherical-porous 3DOM Cu_2O can be proposed. The polymer latex particles carried carboxylate surface groups that interacted strongly with Cu^{2+} ions as well as Cu_2O crystal surfaces, which may induce the preferential Cu_2O nucleation, as the deposition continue, Cu_2O infiltrate quickly through the interstices of the colloidal crystals, where they fill the space evenly to the top to form a level film at −0.35 V shown in Fig. 4a,b which indicated that the Cu_2O product copied the fcc structure of colloidal crystal template to form a perfect 3DOM macroporous material. To everyone knows, the Cu_2O could only be grown in the space between the well-ordered arranged PS spheres, where spatial confined effect played a critical role. When the deposition increased to −0.38 or −0.42 V, it is speculate that the molded Cu_2O went through a nucleation process initiated by an evolving sphere-shaped Cu_2O core formed from an initial ''tuber''. Subsequent growth at the expense of Cu_2O led to its expansion to the top surface of the colloidal crystal. It could be conceived that the morphology evolution of shaped Cu_2O follows a similar way for both the template-free and ordered colloidal crystal templates. Therefore, Cu_2O crystals were grown into cluster shape as freely as on the bare substrate indicating the oxide capital structure itself acts as a key factor. In addition, the deposition depth was deeply influenced by the position of the intersection between PS colloidal crystal and Cu_2O crystalline shown in Fig. 4d labeled A, B, C, the detail will be discussed in the following part.

Figure 5 shows model of side view (perpendicular to (1 1 1) plane) of the colloidal crystal infiltration with different deposition depth. Fig. 5b shows the macroporous film with outermost layer thickness of approximately h = 1/2 r, where r is the radius of the PS spheres used as templates, h is the depth of the outermost layer thickness. The connections between the outermost layer of voids and the layer immediately below are clearly shown by the three darker areas within each void. In addition, the mouths of the voids have a uniform, smooth rounded shape with a diameter of 2r as show in Fig. 3c labeled 3, 4, 5. Fig. 5a presents the macroporous film and the outermost layer thickness is less than r, or other say 1/3r. These correspond to openings from the outer hemispherical void to the three connecting spherical voids in the layer below were broken, which demonstrated a bowl-like feathering as show by arrows in Fig. 3c. Figure 5c reveals the macroporous Cu_2O film in a region where the depth of the outermost layer is 3/4r. As the deposition going on, these interstitial spaces filled in by Cu_2O and pore walls getting thicker than normal. In this case, the diameters of these interconnecting

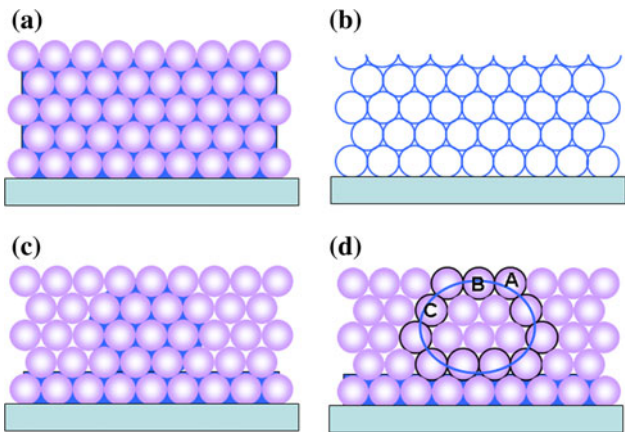

Fig. 4 Schematic illustration of infiltrating process (*side view*, perpendicular to (1 1 1) plane) based on PS colloidal crystal

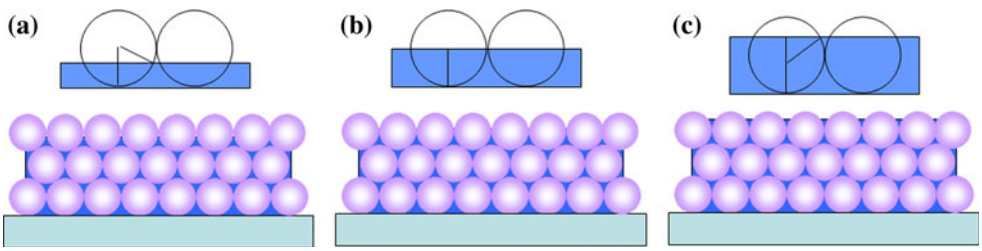

Fig. 5 Models of *side view* (perpendicular to (1 1 1) plane) of the colloidal crystal infiltration with different deposition depth

pore mouths are less than 2r. The image shows that the mouths of the voids have a distorted shape as show in Fig. 3c labeled 7.

4 Conclusion

The fabrication of the perfect 3DOM Cu_2O and their spherical-porous structure was prepared by template assistant electrodeposition via simply adjusting the deposition voltage. The evolution of the surface morphology has been systematically studied. The results demonstrated that the variation of the film morphology due to the electrodeposition infiltrating procedures. The perfect 3DOM Cu_2O film copy well-ordered colloidal crystal templates at −0.35 V. More interestingly, the targets architectures copy both the Cu_2O crystalline and the templates structure at −0.38 or −0.42 V, which is firstly reported systematically. Contemporary, models are set up to discuss the variation of the morphology. When the electrodeposition depth of the outmost layer is 1/2 r, the shape of the pore mouths is round with diameter of 2r. When the depth of the outmost layer is less than 1/2 r, the shape of the pore mouths is imperfect with broken walls. And when the depth of the outmost layer is more than 1/2 r, the distorted pores mouth with thicker wall can be seen.

Acknowledgments This work is supported by the Program National Natural Science Foundation (No. 51010005, No. 51174063 & No. 51102068), the Program for New Century Excellent Talents in University (NCET-08-0168), and Sino-German joint project (GZ550).

References

1. O.D. Velev, A.M. Lenhoff, Curr. Opin. Colloid Interface Sci. **5**, 56 (2000)
2. J. Yu, J.C. Yu, M.K. Leung, W. Ho, B. Cheng, X. Zhao, J. Zhao, J. Catal. **69**, 217 (2003)
3. B.T. Holland, C.F. Blanford, T. Do, A. Stein, Chem. Mater. **11**, 795 (1999)
4. P. Lodahl, A.F. VanDriel, I.S. Nikolaev, A.I. Overgaag, D. Vanmaekelbergh, W.L. Vos, Nature **430**, 654 (2004)
5. S.G. Romanov, A.V. Fokin, L. De, R.M. Rue, Appl. Phys. Lett. **76**, 1656 (2000)
6. S. Jeon, P.V. Braun, Chem. Mater. **15**, 1256 (2003)
7. K. Kanamura, N. Akutagawa, K. Dokko, J. Power Sources **146**, 86–89 (2005)
8. V. Prévot, E. Géraud, T. Stimpfling, J. Ghanbaja, F. Leroux, New J. Chem. **35**, 169–177 (2011)
9. Y.W. Hao, F.Q. Zhu, C.L. Chien, P.C. Searson, J. Electrochem. Soc. **152**, D65–D69 (2007)
10. X.D. Meng, R. Al-Salman, J.P. Zhao, N. Borissenko, Y. Li, F. Endres, Angew. Chem. Int. Ed. **48**, 2703–2707 (2009)
11. J.L. Li, T. Han, N.N. Wei, J.Y. Du, X.G. Zhao, Biosens. Bioelectron. **25**, 773–777 (2009)
12. W.H. Xin, J.P. Zhao, Y.B. Ding, Y. Li, Appl. Surf. Sci. **257**, 10725–10728 (2011)
13. X. Li, Y. Jiang, Z. Shi, Z. Xu, Chem. Mater. **19**, 5424–5430 (2007)
14. Y. Li, W.H. Xin, J.P. Zhao, X.D. Meng, Solid State Sci. **11**, 1625–1630 (2009)
15. M.J. Siegfried, K.S. Choi, Adv. Mater. **16**, 1743–1746 (2004)
16. M.J. Siegfried, K.S. Choi, J. Am. Chem. Soc. **128**, 10356–10357 (2006)
17. C.H. Kuo, M.H. Huang, J. Am. Chem. Soc. **130**, 12815–12820 (2008)
18. X. Li, Y. Jiang, Z.W. Shi, Z. Xu, Chem. Mater. **19**, 5424–5430 (2007)
19. C.M. McShane, K.S. Choi, J. Am. Chem. Soc. **131**, 2561–2569 (2009)
20. J.H. Kim, M. Chainey, M.S. El-Aasser, J.W. Vanderhoff, J. Polym. Sci. A: Polym. Chem. **27**, 3187–3199 (1989)
21. M.A. McLachlan, N.P. Johnson, R.M. RueLaDe, R.M. DeLaRue, D.W. McComb, J. Mater. Chem. **14**, 144–150 (2004)
22. T.D. Golden, M.G. Shumsky, Y. Zhou, R.A. Vanderwerf, R.A. van Leeuwen, J.A. Switzer, Chem. Mater. **8**, 2499 (1996)